Hydraulic adjustments of the Bosphorus exchange flow

T. Oguz

Institute of Marine Sciences, Middle East Technical University, Erdemli, Turkey

Received 4 January 2005; accepted 23 February 2005; published 19 March 2005.

[1] A three dimensional model elucidates connection between observed internal hydraulic characteristics of the Bosphorus flow and channel configuration. A typical two-layer, quasi-steady exchange flow system is shown to be hydraulically adjusted within the strait by a series of morphological features. Three successive hydraulic controls occur within the southern 10 km zone: first near the southern exit due to convex bending of the channel, then at the southern sill and at the constriction. Finally, the exchange flow system experiences another hydraulic control at the northern sill near the Black Sea entrance of the strait. The upper and lower layer flows exiting from the strait at both ends with currents of $\sim$1.0 m s^{-1}, layer depths of $\sim$10 m and $g' \sim 0.1$ ms^{-2} thus impose maximal exchange conditions. **Citation:** Oguz, T. (2005), Hydraulic adjustments of the Bosphorus exchange flow, *Geophys. Res. Lett.*, *32*, L06604, doi:10.1029/2005GL022353.

1. Introduction

[2] The Bosphorus Strait is a long ($\sim$30 km), narrow (<3.0 km), and shallow (<80 m) waterway between the Black and Marmara Seas. It consists of two oppositely flowing currents: the upper layer coming from the Black Sea with a salinity ranging from 18 to 20 psu, and the lower layer coming from the Aegean Sea with a salinity ranging between 36 and 38 psu. In terms of density, the interface covers the sigma-t range of 13–26 kg m^{-3} (Figure 1). The most interesting aspect of the Bosphorus exchange flow system is the anticipated quasi-steady hydraulic controls due to the sills near its two ends and the contraction in the middle. They were qualitatively inferred by abrupt changes of isohalines in these particular regions [*Oguz et al.*, 1990; *Latif et al.*, 1991; *Ozsoy et al.*, 1996; *Di Iorio and Yuce*, 1999; *Ozsoy et al.*, 2001]. The ADCP measurements [*Gregg et al.*, 1999; *Gregg and Özsoy*, 2002] supported the presence of hydraulic control over the northern sill in terms of the two-layer composite Froude number criterion. They however failed to demonstrate controls within the constriction, and the southern sill. *Gregg and Özsoy* [2002] noted possible role of frictional effects for the absence of these controls. Their two-layer composite Froude number computations were however not conclusive because of unavailability of current measurements within $\sim$10 m layers near the surface and the bottom. In fact, studying internal hydraulic characteristics in terms of a two-layer system within the southern one-third of the strait is not entirely appropriate because of the presence of a broad interfacial zone between two homogeneous layers near the surface and the bottom.

0094-8276/05/2005GL022353$05.00

[3] Our objective here is to complement the observational findings by a numerical modeling study, and to arrive at a more refined dynamical understanding of the flow conditions in the southern Bosphorus where the ADCP measurements are of limited use. Taking into account limitations of the layered models [*Oguz et al.*, 1990] we choose to implement here a three dimensional model which accommodates time dependent, continuously stratified flow structure with arbitrary geometry. This model is used to reproduce major flow and stratification characteristics of the Bosphorus, and to identify individual contributions of potentially important lateral and topographical features hydraulically constraining the exchange flow system.

2. Model Description

[4] The three dimensional, time dependent, primitive equations, bottom-following sigma-coordinate Princeton Ocean Model is used in the present study. The vertical mixing is parameterized by the Mellor-Yamada level 2.5 turbulent closure scheme provided as a part of the model code. Rotating 40° clockwise from true north, the x and y coordinates point to along-channel and across-channel directions, respectively, from the origin at its Marmara (southern) side. The along-channel grid distance is 500 m. The across-channel grid distance is 250 m for the idealized straight channel configuration, but reduced to 125 m when the Bosphorus more realistic geometry (Figure 2) is incorporated in the model. 43 km long channel comprises 30 km long actual strait, subsequent 7 km long underwater channel at its northern end, as well as 3 km buffer zones on both sides which are included in order to locate the open boundaries further away from our main region of interest. There are 21 sigma levels in the vertical with finer resolutions near the surface and the bottom. The maximum vertical grid spacing is about 5 m within the deepest section ($\sim$80 m) of the channel. The external and internal time steps are respectively set to 1 s and 60 s.

[5] The two-layer stratification is imposed initially by salinity of 18 psu within the upper 40 m and 38.5 psu at deeper levels. The details of temperature stratification are not important for the present study since the density is mainly governed by salinity variations in the Bosphorus. The temperature is therefore set to 14.5°C for both layers. The normal and tangential velocities are taken as zero at the side walls. At the bottom, adiabatic boundary conditions are specified for temperature and salinity, while a quadratic bottom friction is applied to the momentum flux using the friction coefficient of 0.0025. The horizontal friction, represented in the Laplacian form, uses a constant coefficient of 100 m^2 s^{-1}. The flow structure is however

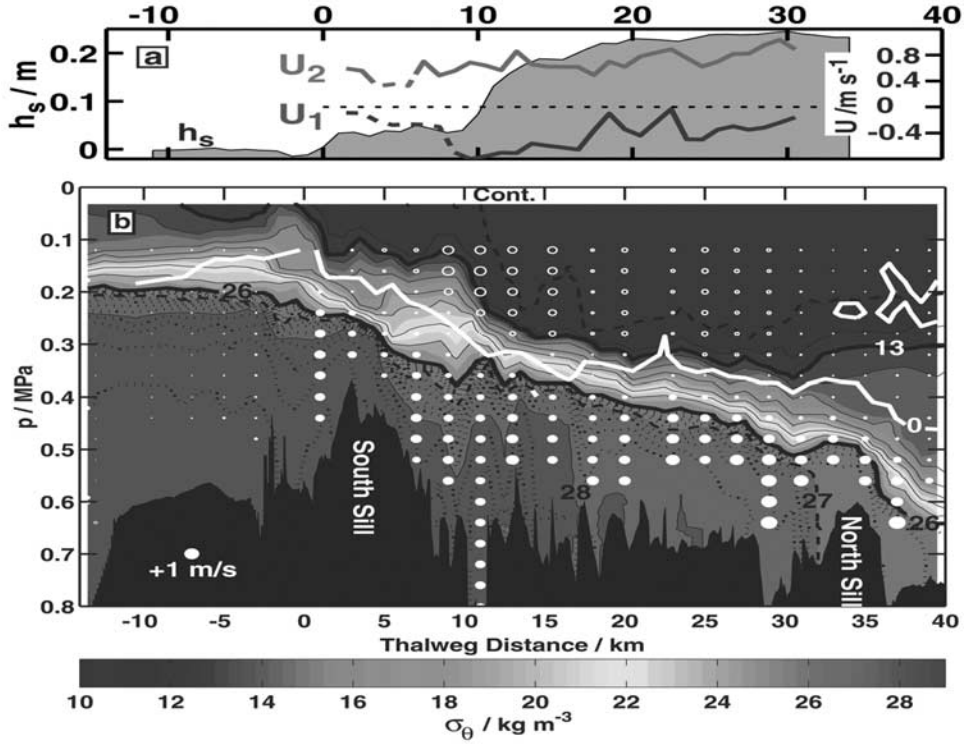

Figure 1. (a) Estimated sea surface height (h_s) and average along-channel currents in the upper (U_1) and lower (U_2) layers, and (b) contours of potential density measured during September 1994. The thick white line shows the zero isotach separating the oppositely flowing upper and lower layer currents. The density interface is shown to confine between 13 and 26 kg m^{-3} sigma-t contours represented by thick dark lines. This figure is taken from *Gregg and Özsoy* [2002].

not sensitive to the choices of these friction coefficients. Wind stress as well as heat and fresh water fluxes were not included.

[6] Forced radiation open boundary conditions are imposed on both sides for the normal velocity component, whereas the tangential velocity component is set to zero. The forced radiation open boundary conditions are adjusted to provide the flow conditions consistent with the observed sea level elevation difference of ~30 cm along the strait as shown in Figure 1. This sea level elevation difference and the subsequent exchange flow system developed within the strait resemble closely the quasi-steady conditions observed earlier by *Oguz et al.* [1990] and others.

[7] Temperature and salinity at both ends of the model domain are prescribed for the inflow conditions, but computed from the adjacent interior values for the outflow conditions. The horizontal advection terms in the salinity and temperature equations are solved by the Smolarkiewicz upstream-corrected scheme, which provides slightly better results with respect to standard centered difference scheme. Model solutions are presented here at the end of seven days of integration, even though steady state was attained after approximately two days of integration.

[8] The layer transports and densities specified at the open boundaries set the density difference between the layers as well as the net barotropic flow through the strait. Then, the layer thicknesses and currents at the anticipated hydraulically controlled exit sections of the strait are simulated by the internal dynamics of the system.

3. Simulations of Hydraulically Controlled Bosphorus Flow Structure

[9] We first consider a simulation using an idealized version of the strait geometry shown in Figure 2. The strait is represented in the form of 2 km wide rectangular channel,

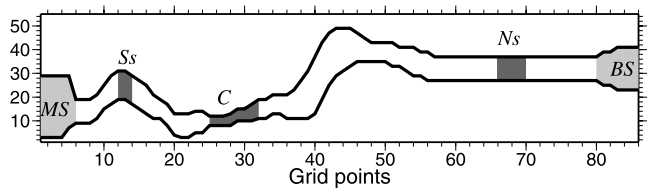

Figure 2. Plan view of the model representation of the Bosphorus Strait. Locations of the southern and northern sills and the contraction zone are indicated by dark gray shaded zones, and the letters Ss, Ns, C, respectively. The actual strait is confined between gridpoints 5 and 63. The northern part of the model domain is extended up to grid point 80 to include the deep channel. The model domain is further extended on both sides by 6 grid points to locate the open boundaries further away from the main region of interest. These regions are shown in gray color with MS and BS indicating the Marmara Sea and the Black Sea, respectively.

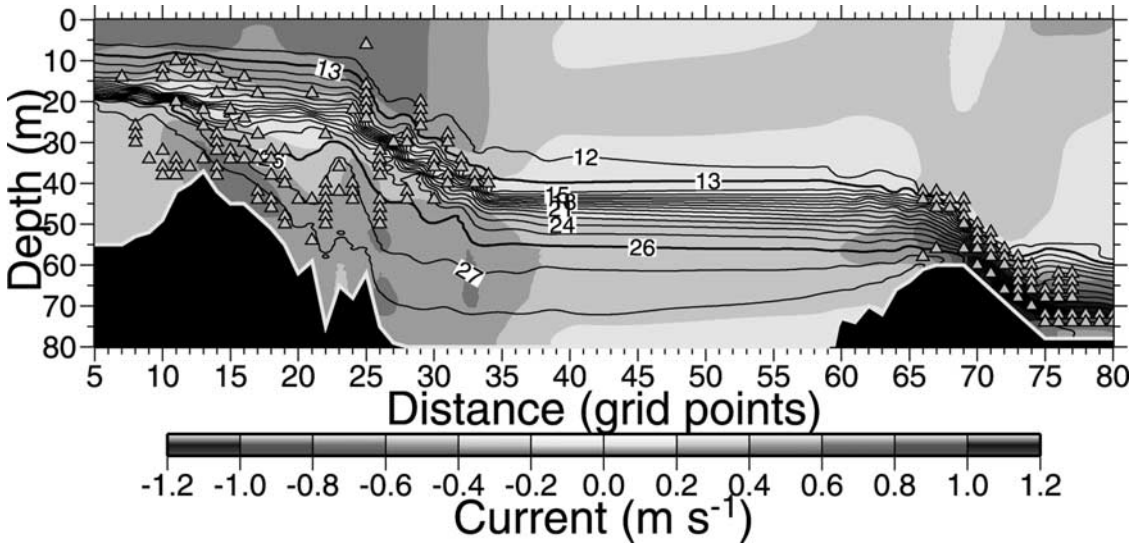

Figure 3. Simulated sigma-t (kg m^{-3}) and horizontal current (m s^{-1}) distributions versus depth along the main axis of the idealized rectangular channel involving the constriction and the southern and northern sills. Sigma-t contours (black lines) are plotted at an interval of 1 kg m^{-3}. The gray color bar gives the current speed with negative (positive) values for the upper (lower) layer. Triangles denote supercritical flow conditions identified by the Richardson number less than 0.25.

in which 4 km long and 1 km wide constriction zone, gradually expanding on its both sides, is placed at 12.5–16.5 km from the Marmara entrance. The idealized channel also accommodates 35–40 m deep southern sill located 3.0–4.0 km away from the Marmara entrance, and 60 m deep northern sill at 2–3 km outside the northern entrance (Figure 1). Variations of the bottom topography between these sills are excluded by taking the flat bottom at 80 m depth.

3.1. Flow and Stratification Characteristics

[10] The flows entering into the channel from both sides quickly establish a two-layer structure shown in Figure 3. The interface, identified by sigma-t range of 13–26 kg m^{-3}, extends almost horizontally at the depth of 47 ± 8 m on the upstream (northern) side of the constriction (Figure 3). Up on entering the constriction zone, the interface rises steeply and linearly by about 25 m, and then extends horizontally at the depth of 16 ± 6 m up to the Marmara end of the channel. The currents in the surface layer are modified accordingly from their values less than 0.5 m s^{-1} to the north of the constriction to about 1.0 m s^{-1} near the southern exit of the constriction, and then to the range of 0.5–0.7 m s^{-1} towards the Marmara end of the channel. The underflow enters into the strait from the Marmara side with salinity of ~38.5 psu, density >28 kg m^{-3} and speed of ~0.3 m s^{-1} below 20 m depth. Currents are then accelerated up to 0.7 m s^{-1}, density is stratified between 26 and 28 kg m^{-3} within the southern sill and constriction zones. Thereafter, the underflow proceeds within the northern half of the strait with weaker currents of about 0.3–0.4 m s^{-1} up to the northern sill, where it undergoes significant transformations. It finally flows with currents in excess of 1.0 m s^{-1} over the sill and on its downstream side within a highly stratified narrow layer. All these features are consistent with the observations (Figure 1). Thus, the simulation with such a highly idealized channel configuration was able to capture very well most of the main observed features of the Bosphorus exchange flow system.

3.2. Internal Hydraulic Characteristics

[11] The limitation of two-layer composite Froude number for identifying internal hydraulic controls is well-known and was often circumvented by introducing interfacial zone as a third layer between the upper and lower layers [*Winters and Seim*, 2000; *Sannino et al.*, 2002]. Similar computations at each cross-section of the strait using two-layer approximation of our simulated multi-level flow structure also suffered from the same deficiency. They only provided the hydraulic control adjustment of the flow at the northern sill. At all other sections, its highest values were about 0.5 observed at the constriction and the southern sill.

[12] For continuously stratified flows, *Pratt et al.* [2000; see also *Smeed*, 2004, section 5] suggested a connection between supercriticality of flows and conditions favorable for mixing; that is the Richardson number being less than 0.25 somewhere in the water column. More rigorous criterion requires solution of the modified Taylor-Goldstein equation for computation of the internal wave phase speeds, as implemented for a simplified case to the Bab al Mandab by *Pratt et al.* [2000]. This approach is however beyond the scope of the present paper. Here, we identify internal hydraulic adjustments only approximately by computing the Richardson number $Ri = [g(\Delta\rho/\rho)\Delta z]/\Delta u^2$ at every two meter bins over the water column.

[13] The condition of $Ri < 0.25$ satisfied at points shown by triangles in Figure 3 indicates transition of the flow to its supercritical state within the constriction. Few grid points beyond its southern exit, the value of Richardson number exceeds its critical limit indicating transition of the flow back to its subcritical conditions. The upper layer plays the major role on this particular hydraulic adjustment of the

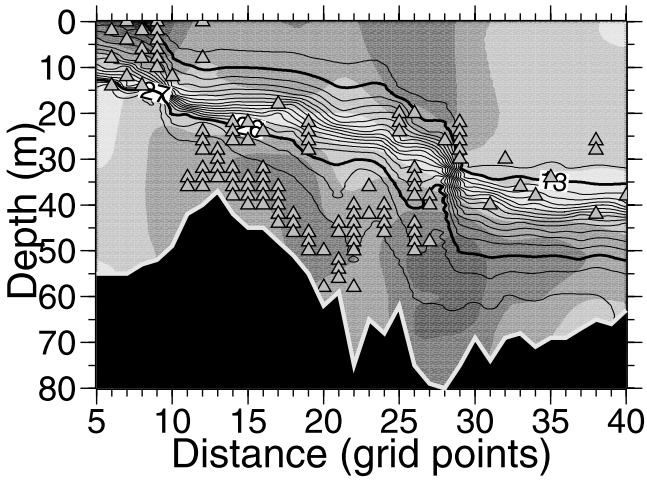

Figure 4. Simulated sigma-t (kg m^{-3}) and horizontal current (m s^{-1}) distributions versus depth along the main axis of the strait shown in Figure 2. Sigma-t contours (black lines) are plotted at an interval of 1 kg m^{-3}, and the scale for current speed given as in Figure 3. Only the southern half of the strait is shown. The flow and stratification characteristics in the northern half are very similar to those shown in the previous figure.

exchange flow system. Its impact on the lower layer is evident by stronger currents, stronger mixing, and a broader zone of weakly stratified water mass structure characterized by 27 and 28 kg m^{-3} sigma-t contours within the deepest 20 m layer of the water column.

[14] Triangles representing $Ri < 0.25$ in Figure 3 indicate another hydraulic control of the exchange flow system over the sill and supercritical conditions on its northern flank, similar to those pointed out theoretically by *Pratt* [1986] and observationally by *Farmer and Denton* [1985]. The mixing associated with this hydraulic adjustment process causes some deformation and broadening of the interface as compared to its fairly stable structure in the northern half of the strait. Sharp rise of the isopycnals at grid point 22–23 and their subsequent deepening at grid points 25–26 indicate establishment of the subcritical state through internal hydraulic jump between two adjacent control sections.

[15] The third hydraulic adjustment takes place when the lower layer flow is sandwiched between the northern sill and the deep upper layer at grid points 67–69. As in the case of the southern sill, the dense water mass of the Mediterranean origin flows supercritically for 3 km along the northern periphery of the sill, and then reverts to the subcritical state through undergoing an internal hydraulic jump. The contribution of the upper layer is negligible for this hydraulic control.

3.3. Contribution of Channel Bends to Hydraulic Control

[16] The idealized-case simulation is repeated using the geometry shown in Figure 2 to introduce (i) a more detailed representation of the constriction zone, (ii) the "L-shape" bends on both sides of the constriction zone, (iii) details of the topography excluded for the region between the sills in the previous simulation. Except slight weakening of currents as compared with the straight channel case, the northern bend does not introduce any appreciable impact on the Bosphorus dynamics. The interface structure, the upper and lower layer flow properties, and the internal hydraulic properties of the exchange flow system between the southern sill and the constriction zone resemble very closely those reported in the previous idealized case (Figure 4). The only major change in the flow structure occurs near the southern end of the strait. The interfacial layer rises gradually and is exposed to another jump around grid points 8–10, which lie on the downstream side of the sharp convex bending of the channel. As suggested by triangles in Figure 4, this jump reflects hydraulic adjustment of the flow, and transition of the upper layer flow to its supercritical state as it leaves the strait with typical currents of about 1.0 m s^{-1} within the uppermost 10 m layer. The lack of these features in the absence of the bend (see Figure 3) shows a contribution of the centrifugal force arising from the channel curvature to the internal hydraulic adjustment of its flow structure near the southern end of the Bosphorus [*Seim and Gregg*, 1997]. No matter how weak, the constriction zone first tilts the interface closer to the surface so that the surface-intensified upper layer flow is able to exert a more strong hydraulic control at the southern exit. As in the previous simulation, the underflow experiences a well-defined control by the sill located near the northern end of the strait. In conclusion, the upper and lower layer flows exiting from the strait at both ends are characterized by $u \sim 1$ m s^{-1}, $h \sim 10$ m, $g' \sim 0.1$ m s^{-2}, and therefore the Bosphorus two-layer exchange flow system possesses the maximal exchange conditions. The way in which the shallow interface at the southern exit is connected to a deeper interface of the Bosphorus-Marmara junction region (Figure 1) in fact reflects an outcome of the maximal exchange.

[17] **Acknowledgment.** We thank two anonymous referees and M. Gregg for their valuable comments.

References

Di Iorio, D., and H. Yuce (1999), Observations of Mediterranean flow into the Black Sea, *J. Geophys. Res.*, *104*, 3091–3108.

Farmer, D. M., and W. A. Denton (1985), Hydraulic control of flow over the sill in Observatory Inlet, *J. Geophys. Res.*, *90*, 9051–9068.

Gregg, M. C., and E. Özsoy (2002), Flow, water mass changes, and hydraulics in the Bosphorus, *J. Geophys. Res.*, *107*(C3), 3016, doi:10.1029/2000JC000485.

Gregg, C. M., E. Ozsoy, and M. A. Latif (1999), Quasi-steady exchange flow in the Bosphorus, *Geophys. Res. Lett.*, *26*, 83–86.

Latif, M. A., E. Ozsoy, T. Oguz, and U. Unluata (1991), Observations of the Mediterranean inflow into the Black Sea, *Deep Sea Res., Part A*, *38*, Suppl. 2, S711–S723.

Oguz, T., E. Ozsoy, M. A. Latif, H. I. Sur, and U. Unluata (1990), Modelling of hydraulically controlled exchange flow in the Bosphorus Strait, *J. Phys. Oceanogr.*, *20*, 945–965.

Ozsoy, E., M. A. Latif, H. I. Sur, and Y. Goryachkin (1996), A review of the exchange flow regimes and mixing in the Bosphorus Strait, in *Dynamics of Mediterranean straits and channels*, *CIESM Sci. Ser. 2*, *Bull. Inst. Oceanogr.*, *17*.

Ozsoy, E., D. Di Iorio, M. C. Gregg, and J. O. Backhaus (2001), Mixing in the Bosphorus Strait and the Black Sea continental shelf: Observations and a model of the dense water outflow, *J. Mar. Syst.*, *31*, 99–135.

Pratt, L. J. (1986), Hydraulic control of sill flow with bottom friction, *J. Phys. Oceanogr.*, *16*, 1970–1980.

Pratt, L. J., H. E. Deese, S. P. Murray, and W. Johns (2000), Continuous dynamical modes in straits having arbitrary cross sections, with applications to the Bab al Mandab, *J. Phys. Oceanogr.*, *30*, 2515–2534.

Sannino, G., A. Bargagli, and V. Artale (2002), Numerical modeling of the mean exchange through the Strait of Gibraltar, *J. Geophys. Res.*, *107*(C8), 3094, doi:10.1029/2001JC000929.

Seim, H. E., and M. C. Gregg (1997), The importance of aspiration and channel curvature in producing strong vertical mixing over a sill, *J. Geophys. Res.*, *102*, 3451–3472.

Smeed, D. A. (2004), Exchange through the Bab el Mandab, *Deep Sea Res., Part II*, *51*, 455–474.

Winters, K. B., and H. Seim (2000), The role of dissipation and mixing in exchange flow through a contracting channel, *J. Fluid Mech.*, *407*, 265–290.

T. Oguz, Institute of Marine Sciences, Middle East Technical University, P. O. Box 28, 33731 Erdemli, Turkey. (oguz@ims.metu.edu.tr)